



Published in final edited form as:

Arterioscler Thromb Vasc Biol. 2019 March ; 39(3): 387–401. doi:10.1161/ATVBAHA.118.311903.

FURIN inhibition reduces vascular remodeling and atherosclerotic lesion progression in mice

Gopala K. Yakala^{1,#}, Hector A. Cabrera-Fuentes^{2,3,4,5,6,#}, Gustavo E. Crespo-Avilan^{2,3,\$}, Chutima Rattanasopa^{1,2,\$}, Alexandrina Burlacu⁷, Benjamin L. George³, Kaviya Anand¹, David Castano Mayan¹, Maria Corliano¹, Sauri Hernández-Reséndiz^{2,3}, Zihao Wu¹, Anne M.K. Schwerk⁸, Amberlyn L.J. Tan¹, Laia Trigueros-Motos¹, Raphael Chevre¹, Tricia Chua¹, Robert Kleemann^{8,9}, Elisa A. Liehn^{3,10,11}, Derek J. Hausenloy^{2,3,12,13,14,15}, Sujoy Ghosh^{2,3,16,*}, and Roshni R. Singaraja^{1,*}

¹Translational Laboratories in Genetic Medicine, A*STAR Institute, and Yong Loo Lin School of Medicine, National University of Singapore, Singapore. ²Cardiovascular and Metabolic Disorders Program, Duke-NUS Medical School, Singapore. ³National Heart Research Institute, National Heart Centre Singapore, Singapore. ⁴Institute of Biochemistry, Medical School, Justus-Liebig-University, Giessen, Germany. ⁵Kazan Federal University, Department of Microbiology, Kazan, Russian Federation. ⁶Tecnologico de Monterrey, Escuela de Ingeniería y Ciencias, Centro de Biotecnología-FEMSA, Nuevo Leon, México. ⁷Institute of Cellular Biology and Pathology “Nicolae Simionescu”, Bucharest, Romania. ⁸The Netherlands Organization for Applied Scientific Research (TNO), Department of Metabolic Health Research, Leiden, The Netherlands. ⁹Department of Vascular Surgery, Leiden University Medical Center, Leiden, The Netherlands. ¹⁰Institute of Molecular Cardiovascular Research, RWTH, Aachen, Germany. ¹¹Human Genetic Laboratory, University of Medicine, Craiova, Romania. ¹²Yong Loo Lin School of Medicine, National University Singapore, Singapore. ¹³The Hatter Cardiovascular Institute, University College London, London, UK. ¹⁴The National Institute of Health Research, University College London Hospitals Biomedical Research Centre, London, UK. ¹⁵Barts Heart Centre, St Bartholomew’s Hospital, London, UK. ¹⁶Biomedical, Biotechnology Research Institute, North Carolina Central University, Durham, USA

Abstract

Atherosclerotic coronary artery disease (CAD) is the leading cause of death worldwide, and current treatment options are insufficient. Using systems-level network cluster analyses on a large CAD case-control cohort, we previously identified proprotein convertase subtilisin/kexin family member 3 (*FURIN*) as a member of several CAD-associated pathways.

Objective: To determine the role of *FURIN* in atherosclerosis.

*Corresponding Authors: Roshni R. Singaraja, 8A Biomedical Grove, Singapore 138648, rsingaraja@tlgm.a-star.edu.sg, T: (65) 6407 4382, F: (65) 6779 4560; Sujoy Ghosh, 8 College Road, Duke-NUS Medical School, Singapore 169857, sujoy.ghosh@duke-nus.edu.sg, T: (65) 66013391.

and \$These authors contributed equally

Disclosures

The authors have declared no conflict of interest.

Approach and results: *In vitro*, FURIN inhibitor treatment resulted in reduced monocyte migration and reduced macrophage and vascular endothelial cell inflammatory and cytokine gene expression. *In vivo*, administration of an irreversible inhibitor of FURIN, α -1-PDX, to hyperlipidemic *Ldlr*^{-/-} mice resulted in lower atherosclerotic lesion area, and a specific reduction in severe lesions. Significantly lower lesional macrophage and collagen area, as well as systemic inflammatory markers were observed. Matrix metalloproteinase 2 (MMP2), an effector of endothelial function and atherosclerotic lesion progression, and a FURIN substrate, was significantly reduced in the aorta of inhibitor treated mice. To determine FURIN's role in vascular endothelial function, we administered α -1-PDX to *ApoE*^{-/-} mice harboring a wire injury in the common carotid artery. We observed significantly decreased carotid intimal thickness, and lower plaque cellularity, smooth muscle cell, macrophage and inflammatory marker content, suggesting protection against vascular remodelling. Over-expression of FURIN in this model resulted in a significant 67% increase in intimal plaque thickness, confirming that FURIN levels directly correlate with atherosclerosis.

Conclusions: We show that systemic inhibition of FURIN in mice decreases vascular remodelling and atherosclerosis. FURIN-mediated modulation of MMP2 activity may contribute to the atheroprotection observed in these mice.

Keywords

Atherosclerosis; Furin; stenosis

Subject codes:

Atherosclerosis; Animal Models of Human Disease

Introduction:

Atherosclerotic coronary artery disease (CAD) is the leading cause of death worldwide¹ and despite improvements in treatment, significant residual disease still remains², prompting the search for new strategies to treat or prevent this illness.

Although the outlines of disease progression are more or less clear, and more recently, a number of genes have been individually implicated in disease pathology, the information gained has not translated into mechanism-based treatments of CAD. Current treatments are largely restricted to controlling risk factors such as hypercholesterolemia and hypertension, but do not directly target mechanisms that drive atherosclerotic processes. The lack of mechanism-based interventions is one reason why the global burden of atherosclerotic cardiovascular disease (ASCVD) continues to rise.

As a first step towards mechanism-based interventions, new approaches to identify putative candidates for therapeutic development are necessary. To this end, we previously conducted a systems analysis of genetic association data from CAD cases and controls (CARDIoGRAM consortium³). Through pathway enrichment analyses, we identified disease-associated pathways that were enriched for CAD-associated polymorphisms in their component genes⁴. One key finding was the identification of a proprotein convertase of the

PCSK subtilisin/kexin family, *FURIN*, as a ‘hub’ gene shared across 6 of 32 replicated CAD-associated pathways⁴, making *FURIN* an attractive target for further validation in atherosclerosis.

FURIN (Proprotein Convertase Subtilisin/Kexin Type 3; *PCSK3*) is a member of the proprotein convertase family that cleave multiple secretory protein precursors at specific single or paired basic amino acids. *Furin* knockout mice die at embryonic day 11, due to cardiac ventral closure defects and hemodynamic insufficiency⁵. However, *Furin*^{+/-} mice are viable, and appear relatively normal, suggesting that ~50% of *FURIN* is sufficient to perform most of its critical functions.

FURIN has been implicated in several diseases. In cancer, treatment with *FURIN* inhibitors reduced various tumors and metastases^{6,7}. *FURIN* expression is increased in the cartilage of patients with osteoarthritis, and treatment of mouse models of arthritis with *FURIN* inhibitors decreased inflammation and arthritis^{8,9}. *FURIN* inhibition also reduced viral infections in *in vitro* models^{10,11}.

FURIN expression is increased in several cell types in human atherosclerotic lesions¹². In addition, *FURIN* expression increased with increasing lesion severity in humans¹³. Liver specific inhibition of *FURIN* in mice led to a decrease in atherosclerotic lesions¹⁴, and *FURIN* levels were correlated with cardiovascular complications in Type 2 diabetics¹⁵. As well, a largescale association analysis identified a single nucleotide polymorphism (SNP), rs17514846, in *FURIN*, as a risk factor for CAD¹⁶. Together, these findings suggest a role for *FURIN* in ASCVD.

A direct investigation of *FURIN* function employing knockout mice models is difficult because mice with targeted deletions in *Furin* die *in utero*⁵. However, chemical and peptide-based *FURIN* inhibitors have been developed and extensively tested in viral and bacterial infections¹⁷, and various types of cancers^{6,18}. These inhibitors show significant efficacy in inhibiting *FURIN* in multiple systems, and are commonly used as tool compounds to probe the function of *FURIN* in cellular and animal models^{19–22}. In this study, we utilize inhibition as well as over-expression of *FURIN in vivo*, and show that systemic *FURIN* levels are directly associated with atherosclerotic lesion progression in mouse models of ASCVD.

Materials and Methods:

The data that support the findings of this study are available from the corresponding author upon reasonable request. Please see the Major Resources Table in the Supplemental Material.

Pathway enrichment and Gene Expression Omnibus analyses

To identify novel associations between established biological mechanisms and CAD, we carried out a 2-stage pathway-based gene-set enrichment analysis of 16 genome-wide association study (GWAS) data sets for CAD (available through the CARDIoGRAM consortium). Pathway enrichment analysis was conducted via the i-GSEA4GWAS (<http://gsea4gwas.psych.ac.cn/inputPage.jsp>) tool²³ by querying the Reactome pathway database²⁴.

From a meta-analyzed discovery cohort of 7 CAD GWAS data sets (9,889 cases/11,089 controls), nominally significant pathways were tested for replication in a meta-analysis of 9 additional studies (15,502 cases/55,730 controls).

To examine *FURIN* gene expression levels in atherosclerosis-relevant samples from human sources, we screened the Gene Expression Omnibus (GEO) for human studies identified by the keywords ‘macrophages’, ‘vascular endothelial cells’, ‘vascular smooth muscle cells’, and ‘atherosclerotic plaques’. 18 microarray studies (Affymetrix and Illumina platforms), encompassing 570 samples were ultimately retrieved and analyzed. We queried the expression of *FURIN* and other proprotein convertases in samples from the different biological sources. To enable comparisons between diverse GEO datasets, the expression values from each study were converted into quintiles with Q1 representing the upper 20% and Q5 the bottom 20% of all expression values.

Western-type diet fed *Ldlr*^{-/-} model of atherosclerosis

All experiments were approved by the Biomedical Sciences Institute (BMSI) Singapore Institutional Animal Care Committee and adhered to the “Recommendation on Design, Execution, and Reporting of Animal Atherosclerosis Studies” by the American Heart Association²⁵. Thirty-two male *Ldlr*^{-/-} mice (C57BL/6JInv, Jackson Laboratory) on a 12h light-dark cycle were maintained on chow diet (1324_modified, Altromin GmbH & Co.) until 12 weeks of age, followed by a western type diet (WTD; D12079B, Research Diets, NJ) for 8 weeks. Half the mice were injected intra-peritoneally with 1xPBS, and the other half with 100 µg/kg of *FURIN* inhibitor (α-1-PDX, RP-070, Thermo-Fisher scientific), twice per week, for 8 weeks in conjunction with the WTD feeding. The mice had free access to food and water except during a 4–5 h fast period prior to blood sample collection. Mice were anesthetized at 20 weeks (100mg/kg ketamine hydrochloride/10mg/kg xylazine i.p.), bled retro-orbitally, perfused transcardially with 1xPBS, and hearts fixed in 4% paraformaldehyde (Sigma) and embedded in paraffin. Livers, aortic arch and thoracic aorta were snap frozen in liquid N₂ and stored at –80°C.

Plasma *FURIN*, inflammatory markers and lipid quantification

Plasma HDL cholesterol (HDLc), LDL cholesterol (LDLc) and triglycerides were measured by COBAS analyzer (c111, Roche), using kits 05401488, 05401682 and 04657594 (Roche Diagnostics, Switzerland), respectively. Plasma *FURIN* (E9700m, Wuhan EIAab Science, China), IL1-β, TNF-α and TGF-β (R&D Systems, USA) were determined by ELISA following manufacturer’s instructions.

Atherosclerotic lesion analyses

Serial cross sections (5µm-thick) were taken throughout the entire aortic root for histological analyses as described^{26,27}. Briefly, aortic cross-sections were stained with hematoxylin-phloxine-saffron and atherosclerotic lesion area was analyzed in 4 cross-sections/mouse. Aperio Imagescope (Leica Biosystems, USA) and ImageJ were used for morphometric quantification of lesion number, area and severity according to the American Heart Association^{26,27} classification. MAC-3 (550292, BD-Pharmigen, USA) and α-SMA (61001, Progen, Germany) antibodies were used to determine macrophage and smooth muscle actin

content. Sections were stained with Picrosirius red (365548, Sigma, USA) for collagen content.

Matrix metallopeptidase activity assays

The aortic arch was dissected, snap frozen and homogenized in RIPA buffer. Twenty μ g protein was mixed with SDS-Tris-glycine sample buffer without a reducing agent, loaded onto a pre-cast 10% SDS-polyacrylamide gel containing 1 mg/mL gelatin (EC6175BOX, Thermo-Fisher scientific, USA) and samples electrophoresed according to manufacturer's protocol (Thermo-Fisher scientific, USA). Mouse recombinant MMP2 (554402, Biolegend, USA) and MMP9 (755202, Biolegend, USA) were used as positive controls. Digested bands were quantified by ImageJ software.

Carotid artery wire injury model of vascular remodelling

Male, 10–12 week old *Apoe*^{-/-} mice (C57BL/6J background) from Charles River Laboratory (Italy) maintained on 12 hr dark/light cycle and fed an atherogenic high fat diet (HFD, 21% fat, 0.15% cholesterol, Altromin) for 1 week before and 2 weeks after injury, were anaesthetized (100 mg/kg ketamine hydrochloride/10mg/kg xylazine i.p.) and subjected to endothelial denudation of the left common carotid artery by a 1 cm insertion of a flexible 0.36-mm guide wire through a transverse arteriotomy of the external carotid artery, as described²⁸. For the inhibitor studies, *Apoe*^{-/-} mice were continuously treated with FURIN inhibitor α -1-PDX (20 μ g/kg per day) via Alzet® osmotic minipumps, subcutaneously implanted one day before injury. For the recombinant FURIN expression studies, 2 units of purified human recombinant FURIN (P8077, New England Biolabs, MA, USA) in 20 nM HEPES per mouse was injected three times per week, intraperitoneally, beginning on the day of wire injury. At 2 weeks after injury, the mice were sacrificed and perfused *in situ* with 4% paraformaldehyde. The injured carotid arteries were isolated, fixed in 4% paraformaldehyde, dehydrated and embedded in paraffin. Serial 4 μ m transverse sections (9 sections/mouse, 40 μ m apart) were collected within a distance of 0 to 320 μ m from the bifurcation, stained using Elastica-van Gieson (EVG) and areas of lumen, neointima (between lumen and internal elastic lamina), and media (between internal and external elastic laminae) were measured by planimetry using Diskus Software (Hilgers). For each mouse, data from the 9 sections were averaged to represent lesion formation along this standardized distance. Neointimal macrophages, smooth muscle cells and endothelial cells were visualized by immunofluorescence staining for MAC2 (M3/38, Cedarlane), SMA (1A4, Dako) or CD31 (M-20, Santa Cruz Biotechnology), respectively, followed by FITC- or Cy3-conjugated secondary antibody staining (Jackson ImmunoResearch) as described^{29,30}. Animal studies were approved by local authorities and complied with German animal protection law and also approved by the Biomedical Sciences Institute (BMSI) Singapore Institutional Animal Care Committee.

Cell culture and differentiation

THP-1 cells were differentiated using 10ng/mL phorbol 12-myristate-13-acetate (PMA, Sigma-Aldrich) for 48h, then in RPMI1640 (10% FCS, 1% L-glutamine) for 24 h. For experiments with THP-1-activated monocytes, cells were stimulated with 100ng/mL of LPS (LPS-EB Ultrapure, InvivoGen) for 4h. FURIN activity assays were performed in THP-1

monocytes and PMA-differentiated macrophages after 24h incubation in the absence or presence of LPS (100 ng/ml) following manufacturer's instructions (New England Biolabs).

Primary human coronary artery endothelial cell line (HCAEC) from ATCC (Manassas, VA) were cultured in EndoGRO-VEGF Complete Culture Media (Merck, Kenilworth, NJ) supplemented with 20% FBS, heparin, endothelial cell growth factor, nonessential amino acids, and antibiotics. 1×10^5 HCAEC cells were placed in 12 well plates and treated with 25 μ M Decanoyl-RVKR-CMK (dec-CMK, Merck), recombinant human TNF- α (20 ng/ml, BioLegend), or dec-CMK followed by TNF- α .

Real-time RT-PCR

Total RNA was prepared using NucleoSpin® RNA Mini kit (Macherey-Nagel) and cDNA was synthesized using iScript™ cDNA Synthesis Kit (Bio-RAD). Real-time PCR analyses were performed on an Applied Biosystems Viia 7 instrument, with PrecisionFAST™ 2X qPCR Mastermix (PrimerDesign). PCR runs included a 2 min pre-incubation at 95°C, followed by 50 cycles consisting of 95°C for 5s, 64°C for 5s and 72°C for 10s. After completion of PCR a melting curve and Cq value were analyzed. Primer sequences are available upon request.

Statistical analyses

Data were analyzed using GraphPad prism (Prism version 7, GraphPad Software, USA). D'Agostino's K^2 and Shapiro-Wilk tests were applied to determine the normality of the data. If the data passed the normality tests, differences between two groups were analyzed using Student's T-test. If data did not pass normality, Mann-Whitney tests were applied to check for significant differences. One-way ANOVA was used to determine the significant differences for multiple group comparisons, followed by a Tukey's post hoc test. For non-parametric multiple comparisons, Kruskal-Wallis tests were used. Dose-response curves of FURIN activity in cultured cells were generated via the *drc* software in R, based on a 4-parameter log-logistic model³¹. Values of $p < 0.05$ were considered to represent significant differences between groups. Results are shown as mean \pm SEM.

Results:

Genetic and genomic evidence support a role for *FURIN* in atherosclerosis

Pathway enrichment analyses of genome-wide association studies had previously identified 32 Reactome pathways as replicably associated with CAD⁴. Analyses of pathway inter-relationships via sharing of gene components identified FURIN as a central component of 6 CAD-associated Reactome pathways³², including degradation of the extracellular matrix, extracellular matrix organization, post-translational modification (gamma carboxylation, hypusine formation and arylsulfatase activation), signaling by platelet-derived growth factor (PDGF), signaling by NOTCH, and signaling by transforming growth factor beta (TGF- β) receptor complex (Fig 1a). These findings suggest a possible role for FURIN in vascular remodeling (via extracellular matrix modulation³³ and PDGF signaling pathways³⁴), inflammation and cellular infiltration (via Notch and PDGF signalling^{34,35}), and regulation of plaque stability (via TGF- β signalling³⁶), thereby affecting both early and late-stage

atherosclerotic processes. To evaluate additional evidence for FURIN's potential involvement in atherosclerosis, we screened large-scale gene expression data from the Gene Expression Omnibus (GEO)³⁷ for human studies relevant to atherosclerosis, from which 18 microarray studies encompassing 570 samples were retrieved and analyzed. *FURIN* was highly expressed in all atherosclerosis-relevant cell-types (Fig 1b) and in atherosclerotic plaques. Of all proprotein convertases tested, *FURIN* expression was most consistently high in all atherosclerosis relevant cell-types, including plaques. This finding is also consistent with other published data showing high *FURIN* levels in atherosclerotic plaques³⁸.

FURIN inhibition decreases monocyte migration and monocyte/macrophage and vascular endothelial inflammatory gene expression *in vitro*.

Since our Reactome pathway analyses suggested a potential role for FURIN in inflammation and cellular infiltration, we first assessed if FURIN plays a role in monocyte migration. Dose-response curves for FURIN inhibition in monocytes, macrophages and human coronary artery endothelial cells were determined by treating cells with varying concentrations of the irreversible, cell permeable and competitive FURIN inhibitor Decanoyl-RVKR-CMK³⁹ (Supp Figure I). In transwell migration assays, the migration of lipopolysaccharide (LPS) activated monocytes was significantly decreased in the presence of Decanoyl-RVKR-CMK (Fig 2a), demonstrating that FURIN facilitates the transmigration of monocytes. The decreased number of transmigrated monocytes was not a result of increased cell death in the inhibitor treated group (Fig 2b). To determine the impact of FURIN inhibition on inflammatory and adhesion molecule expression, we assessed gene expression levels. In monocytes, the expression of the adhesion molecule *VCAM-1* was significantly reduced in the presence of the inhibitor (Fig 2c). No changes were observed in the expression of the inflammatory markers *CCL2*, *NF- κ B* and *IL-1 β* , as well as the adhesion molecule, *ICAM-1* (Fig 2c). Under LPS stimulated inflammatory conditions in monocytes, a significant inhibition of *ICAM-1* and *IL-1 β* expression was observed (Fig 2d), suggesting that FURIN inhibition may reduce monocyte inflammatory cytokine and adhesion molecule expression during atherogenesis. In macrophages, the expression of *CCL2*, *VCAM-1* and *ICAM-1* were all reduced in the presence of the FURIN inhibitor (Fig 2e), suggesting that inflammatory chemokine, cytokine and adhesion molecule expression may also be significantly decreased by FURIN inhibition in lesional macrophages. We next assessed the response of FURIN to LPS elicited inflammation, and found a significant decrease in macrophage FURIN activity (Fig 2f). This decrease in FURIN activity was not observed in monocytes upon LPS stimulation (Fig 2f). Together, these data show that FURIN modulates monocyte recruitment and trans-migration, and regulates monocyte and macrophage response to inflammatory stimulation.

We next assessed the impact of FURIN inhibition on TNF- α stimulated vascular endothelial cells, since FURIN is expressed in and plays a critical role in endothelial cell function⁴⁰. A significant reduction in *NF- κ B*, *CCL2*, *IL-1 β* and *VCAM-1* expression was observed (Supp Fig II), whereas no changes in *ICAM-1* expression were observed. These data suggest that FURIN inhibition may protect against inflammatory stimulation in both monocyte/macrophages and vascular endothelial cells during atherosclerosis.

Lower plasma FURIN levels in FURIN inhibitor treated mice

Since our *in silico* analyses showed *FURIN* to be a hub gene in CAD-associated pathways, its levels were elevated in atherosclerotic plaques, and our *in vitro* studies suggested FURIN inhibition may be atheroprotective, we next assessed if FURIN plays a role in atherosclerotic lesion development *in vivo*. We utilized α -1-PDX, a peptide inhibitor of FURIN that functions as a suicide substrate that irreversibly binds to and causes the degradation of the FURIN protein^{21,41}. Male, 12 week old *Ldlr*^{-/-} mice on a western type diet (WTD) were injected thrice per week intra-peritoneally with the FURIN inhibitor for 8 weeks. To determine if FURIN inhibitor treatment has an effect on FURIN protein levels *in vivo*, we quantified plasma levels of FURIN in inhibitor treated and vehicle treated control mice. Compared to controls, circulating plasma levels of FURIN were significantly lower (59% decrease, $p=0.002$) in the FURIN inhibitor treated mice, suggesting that indeed, administration of the FURIN inhibitor α -1-PDX resulted in reduced circulating FURIN levels (Supp Fig IIIa).

Lower atherosclerotic lesion area and severity in FURIN inhibitor treated *Ldlr*^{-/-} mice

To determine the impact of FURIN inhibition on atherosclerotic lesion development, the WTD fed *Ldlr*^{-/-} mouse model was utilized⁴². Atherosclerotic lesions were analyzed after 8 weeks of concurrent WTD and α -1-PDX administration, in hematoxylin phloxine saffron (HPS) stained sections of the aortic sinus. A trend toward lower total lesion area in the FURIN inhibitor treated group was observed (FURIN inhibitor: 39.87 ± 5.51 ; Control: $50.07 \pm 6.40 \times 10^3 \mu\text{m}^2$, $n=15$ each, $p=0.2$) (Figs 3a and b). Lesions were then categorized using the American Heart Association (AHA) classification system as mild (class I to III) or severe (classes IV and V)^{26,27}. No change in the area of mild lesions was observed (FURIN inhibitor: 43.22 ± 9.99 ; Control: $38.19 \pm 8.43 \times 10^3 \mu\text{m}^2$, $n=15$ each, $p=0.7$) (Figs 3c and d). However, significantly lower (by 66%) advanced lesion area was observed in the FURIN inhibitor treated group (FURIN inhibitor: 14.43 ± 6.26 ; Control: $42.03 \pm 11.87 \times 10^3 \mu\text{m}^2$, $n=15$ each, $p=0.04$) (Fig 3d) suggesting that in the *Ldlr*^{-/-} hypercholesterolemic model, FURIN inhibition reduced the formation of more mature lesions.

FURIN inhibition reduces atherosclerotic lesion complexity

Since an overall trend to lower lesion area, and a significant decrease in advanced lesion area was observed in FURIN inhibitor treated mice, we next assessed lesion complexity. Significantly lower (by 34%) macrophage (MAC3) positive lesion area was observed in the FURIN inhibitor treated mice (FURIN inhibitor: 102.69 ± 16.45 , $n=14$; Control: 155.09 ± 12.50 , $n=15$, $\times 10^3 \mu\text{m}^2$, $p=0.04$) (Figs 3e and f). The smooth muscle cell area of lesions, assessed by α -smooth muscle actin immunostaining did not significantly differ between the groups (FURIN inhibitor: 46.43 ± 7.72 , $n=13$; Control: 54.36 ± 5.79 , $n=14$, $\times 10^3 \mu\text{m}^2$, $p=0.4$) (Supp Figs IIIb and c), suggesting that FURIN inhibition, in this model, did not decrease plaque cellularity. In addition, Picrosirius red staining showed a significantly lower area of thick mature collagen fibers in lesions (FURIN inhibitor: 72.34 ± 7.91 ; Control: $109.19 \pm 13.59 \times 10^3 \mu\text{m}^2$, $n=15$ each, $p=0.02$) (Figs 3g and h), suggesting reduced lesional collagen in FURIN inhibitor treated mice.

FURIN inhibition reduces systemic inflammation in mice

Since treatment of the western-type diet fed *Ldlr*^{-/-} mice with α -1-PDX resulted in reduced advanced lesion size and complexity, we next assessed levels of circulatory markers of inflammation in the mice. Plasma levels of the inflammation marker TNF- α were 44% lower in FURIN inhibitor treated mice (FURIN inhibitor: 21.6 ± 3.1 , n=15; Control: 38.8 ± 7.5 , n=14, pg/ml, p=0.05) (Fig 4a). Similarly, plasma levels of the inflammation marker IL1- β were also significantly lower (by 66%) in the FURIN inhibitor treated group (FURIN inhibitor: 13.9 ± 2.8 , n=15; Control: 40.8 ± 8.9 , n=14, pg/ml, p=0.01) (Fig 4b). Furthermore, we assessed levels of active TGF- β 1, an inflammatory cytokine that plays a critical role in extra cellular matrix degradation, which is also a substrate for FURIN⁴³. Active TGF- β 1 levels were significantly lower in the FURIN inhibitor treated mice (FURIN inhibitor: 45.8 ± 5.1 , n=16; Control: 62.0 ± 4.6 , n=15, pg/ml, p=0.02) (Fig 4c), in line with our finding of lower lesional collagen in FURIN inhibitor treated mice.

FURIN inhibitor treatment results in elevated plasma HDL-cholesterol levels

Low levels of plasma apolipoprotein B-containing lipoproteins are associated with atheroprotection, both in humans and in mice⁴⁴. To determine if lipid levels were altered in the FURIN inhibitor treated hyperlipidemic *Ldlr*^{-/-} mice, we quantified plasma lipids. Plasma LDL-cholesterol (FURIN inhibitor: 28.4 ± 1.9 ; Control: 24.6 ± 1.9 mmol/L, n=16 each, p=0.1) and triglycerides (FURIN inhibitor: 7.6 ± 0.5 ; Control: 7.7 ± 0.7 mmol/L, n=16 each, p=0.9) did not differ significantly between the groups (Supp Figs IVa and b). However, HDL cholesterol (HDLc) levels were significantly elevated in the FURIN inhibitor treated mice (FURIN inhibitor: 7.4 ± 0.2 ; Control: 6.6 ± 0.1 mmol/L, n=16 each, p=0.005) (Fig 4d).

FURIN inhibition reduces matrix metallopeptidase activation

As a proprotein convertase, FURIN promotes the conversion of Pro-MMP2 to MMP2 via MT-1 MMP activation⁴⁵. In addition, the absence of MMP2 results in significant decreases in atherosclerotic lesions in *Mmp2*^{-/-} \times *ApoE*^{-/-} mice⁴⁶. Thus, we hypothesized that the inhibition of FURIN may have reduced atherosclerotic lesion progression in part via the inhibition of MMP2 activity. Indeed, as assessed by gelatin zymography⁴⁷, levels of total MMP2 (FURIN inhibitor: 3530 ± 749 ; Control: 11580 ± 1919 densitometry arbitrary units, n=7 each, p=0.002) (Figs 4e and f), and active/pro-MMP2 (FURIN inhibitor: 0.043 ± 0.01 ; Control: 0.18 ± 0.04 arbitrary units, n=7 each, p=0.01) (Figs 4e and g) were significantly decreased in the aortic arch of FURIN inhibitor treated mice. Although not shown to be a substrate for FURIN cleavage, MMP9 plays a role in atherosclerosis development⁴⁸, and deficiency of MMP9 reduced atherosclerotic lesions in mice⁴⁹. We observed no changes in MMP9 levels in the aortic arch of FURIN inhibitor treated mice (FURIN inhibitor: 7359 ± 1435 ; Control: 5482 ± 542 arbitrary units, n=7 each, p=0.24) (Supp Fig V), suggesting that FURIN inhibition reduced atherosclerotic lesions in part via the modulation of MMP2 but not MMP9 activity.

Lower intima thickening and plaque area in FURIN inhibitor treated *ApoE*^{-/-} mice

Since our *in silico* genetic association and gene expression analyses implicated FURIN as a possible mediator of vascular remodelling in atherosclerosis, and MMP2 plays an important

role in subendothelial basement membrane formation⁵⁰, we next assessed the impact of FURIN inhibition in a wire injury model of vascular remodelling and restenosis. We administered α -1-PDX FURIN inhibitor via transplanted osmotic mini pumps to western type diet fed *Apoe*^{-/-} mice in which the endothelium of the common carotid artery was injured with a flexible wire, an established model for the study of vascular remodeling in atherosclerosis⁵¹. Intimal lesions at the denuded regions were assessed in control and FURIN inhibitor treated mice. Significantly lower (by 54%) intimal thickness (FURIN inhibitor: 34.1 ± 7.2 ; Control: $73.9 \pm 7.4 \times 10^3 \mu\text{m}^2$, n=6, p=0.003) as well as total plaque area (by 35%) (FURIN inhibitor: 85.7 ± 11.0 ; Control: $131.5 \pm 15.9 \times 10^3 \mu\text{m}^2$, n=6, p=0.04) were observed in the FURIN inhibitor treated mice (Figs 5a–d), suggesting that inhibition of FURIN resulted in significant protection from vascular restenosis and lesion formation in this mouse model.

Lower plaque cellularity, macrophage number and inflammation in FURIN inhibitor treated mice

To determine if, in addition to the reduced lesion area, FURIN inhibition also resulted in reduced lesional macrophage number and inflammation, we assessed these parameters in the *Apoe*^{-/-} wire injury model *in vivo*. Levels of the inflammatory marker TNF- α in the plaque were significantly lower (FURIN inhibitor: 17.5 ± 2.0 ; Control: 25.8 ± 2.4 arbitrary units/ μm^2 , n=6 each, p=0.02) (Fig 5e) suggesting that FURIN inhibition reduces plaque inflammation. Levels of the endothelial adhesion molecule ICAM-1 were not changed in FURIN inhibitor treated mice (Fig 5f). Total cell number (FURIN inhibitor: 178.6 ± 25.6 ; Control: 438.2 ± 45.0 , cells/plaque, n=6 each, p<0.0001) (Fig 6a), smooth muscle cell number (FURIN inhibitor: 22.4 ± 3.7 ; Control: 54.2 ± 6.3 cells/plaque, n=6 each, p=0.0001) (Fig 6b), and macrophage (MAC-2⁺) number (FURIN inhibitor: 74.9 ± 13.5 ; Control: 127.5 ± 16.8 cells/plaque, n=6 each, p=0.02) (Fig 6c) were significantly lower in atherosclerotic lesions of FURIN inhibitor treated mice. No significant differences in plaque endothelial cell numbers (CD31⁺) were observed (Fig 6d). Negative control isotype-specific immunoglobulin staining for these antibodies are shown in Supp Fig VI. These data show that FURIN inhibition *in vivo* reduces plaque cellularity, macrophage numbers and plaque inflammation.

Increased FURIN expression increases plaque area in *Apoe*^{-/-} mice

Our experiments thus far utilized a FURIN inhibitor, α -1-PDX, to determine the impact of reducing FURIN levels on atherosclerotic lesion development *in vivo*. However, although this inhibitor shows significant efficacy in inhibiting FURIN, it is not entirely selective against FURIN^{19,20}. To more directly confirm the role of FURIN in atherosclerotic lesion development, we next administered purified FURIN protein into WTD fed *Apoe*^{-/-} mice harboring a wire injury of the common carotid artery as described above. Significantly higher intimal thickness (FURIN: 126.50 ± 8.91 ; Control: $75.59 \pm 11.05 \times 10^3 \mu\text{m}^2$, n=5–6, p=0.005) as well as total lesion area (FURIN: 172.63 ± 7.82 ; Control: $117.57 \pm 12.45 \times 10^3 \mu\text{m}^2$, n=5–6, p=0.004) were observed in the lesions at the denuded regions of the carotid in the FURIN over-expressing mice (Fig 7a–c), confirming that FURIN levels are directly associated with vascular remodeling and lesion development. In addition to intimal lesion area and thickness, we also assessed macrophage and smooth muscle content in the lesions

of these mice. A significant increase in lesional smooth muscle area was observed (FURIN: 51.01 ± 5.33 ; Control: $32.58 \pm 4.66 \times 10^3 \mu\text{m}^2$, $n=18-19$, $p=0.01$) (Fig 7d). However, no changes in lesional macrophage (MAC-2⁺) area (FURIN: 23.40 ± 2.50 ; Control: $24.69 \pm 3.80 \times 10^3 \mu\text{m}^2$, $n=18-19$, $p=0.77$) (Fig 7e) were observed.

Discussion:

We show here that levels of the Proprotein Convertase FURIN are directly associated with atherosclerosis and restenosis, both in the hyperlipidemic *Ldlr*^{-/-} model of atherosclerosis, as well as in a carotid wire injury model of vascular endothelial remodelling. We find that systemic inhibition of FURIN prevented atherosclerosis progression in mice, in part through the modulation of MMP2 activity.

In our *Ldlr*^{-/-} mice, a significant reduction in severe lesions with no changes in early lesions were observed after FURIN inhibition, suggesting that FURIN might play a role in the later stages of lesion development. This is in line with the finding that *FURIN* was the most dysregulated primary PCSK in advanced atherosclerotic plaques, with a median RNA overexpression of ~40-fold compared to non-atherosclerotic control samples³⁸. As well, later stage, rupture-prone atherosclerotic lesions contain activated MMPs including MMP2⁵² that weaken the plaque cap via extracellular matrix degradation^{52,53}. MMP2 is a FURIN substrate, and is activated by FURIN⁴⁵. Thus, the prevention of vascular MMP2 activation via FURIN inhibition may attenuate the development of severe lesions.

It is possible that reduced MMP2 levels are not the sole mechanism underlying the atheroprotective phenotypes we observe in the face of FURIN inhibition, since FURIN has many protein substrates. However, *Mmp2*^{-/-} mice, when crossed to the *Apoe*^{-/-} mice, show a significant reduction in atherosclerotic lesions at the aortic sinus, as well as significantly reduced macrophage and collagen content in aortic sinus lesions⁴⁶, similar to our findings in the FURIN inhibitor treated mice. In addition, no changes were observed in MMP9 levels in the *Mmp2*^{-/-} × *Apoe*^{-/-} mice⁴⁶, similar to our findings that MMP9 levels are unaltered in the aortic arch of the FURIN inhibitor treated mice. The reduced systemic inflammatory markers observed in the face of FURIN inhibition in our mice could also be modulated via the inhibition of MMP2 activity, since the chemokine ligands CCL7 and CXCL-12 are substrates for MMP2^{54,55} and *Mmp2*^{-/-} mice display reduced allergic inflammation⁵⁶ suggesting a direct role for MMP2 in modulating inflammation.

The curated FURIN substrate database, FurinDB (<http://www.nuolan.net>) lists 87 mammalian substrates for FURIN⁵⁷. These include many proteins with functions in the extracellular matrix, suggesting that one mechanism by which FURIN inhibition may reduce atherosclerotic lesions is via the regulation of the extracellular matrix, which plays a central role in tissue remodelling, as well as cell migration, cytokine and chemokine recruitment, and adhesion receptor and cell surface proteoglycan recruitment at sites of lesions³³. In line with a central role for FURIN in tissue remodelling, our data show that FURIN inhibition had a significant impact in reducing lesions in our model of vascular endothelial injury induced atherosclerosis.

Of interest, FURIN is a protease for pro-protein convertase subtilisin/kexin type 9 (PCSK9)⁵⁸, a critical regulator of LDL cholesterol (LDLc) metabolism, with an established role in atherosclerosis⁵⁹. The accepted mechanism at present for PCSK9's role in LDLc metabolism and atherosclerosis is directly related to its role in the LDL receptor (LDLR) pathway. PCSK9 binds to LDLRs at the plasma membrane and targets them to lysosomes for degradation⁶⁰. Since PCSK9 is a substrate for FURIN, to exclude a contribution by PCSK9 in our analyses of atherosclerosis, we chose the *Ldlr*^{-/-} mouse model for part of our experiments. In addition, we saw no changes in plasma LDLc levels in our experiments. However, more recent studies on PCSK9 suggest that it may act in a paracrine manner in the arterial wall⁶¹. Thus, if PCSK9 might modulate atherosclerosis through LDLR independent mechanisms, and if FURIN might play a role in these mechanisms is unclear.

One potential caveat to our study was considered, which is the substrate specificity of the FURIN inhibitor, α -1-PDX. The α -1-PDX inhibitor was generated by mutating the reactive-site loop of α -1-antitrypsin to contain the minimal consensus sequence for FURIN cleavage⁶², resulting in the generation of a SDS-resistant complex with FURIN through its catalytic serine⁶². α -1-PDX displayed high selectivity for FURIN with K_i values as low as 600 pM⁴¹. However, at higher concentrations, α -1-PDX can also inhibit PC5/6⁴¹. If PC5/6 plays a role in atherosclerosis is unknown. As PC5/6 is expressed predominantly in the small intestine, kidney and lung of adult mice⁶³, a direct effect of PC5/6 in atherosclerosis is unlikely. Despite the partial non-specificity of α -1-PDX, in biochemical, cellular and animal studies, α -1-PDX is well established to block FURIN activity⁶⁴. To exclude the possibility that other proteins inhibited by α -1-PDX may have caused the observed reduction in atherosclerotic lesions in our experiments, and to directly confirm that FURIN alone can modulate atherosclerotic processes, we delivered FURIN protein to mice with a vascular endothelial injury in their carotid arteries and found a 67% increase in intimal lesion area in the face of FURIN over expression, directly implicating a role for FURIN in lesion formation. Of note, the ATVB Council recommends the use of both sexes in studies of atherosclerosis⁶⁵. Only male mice were utilized here, which is a limitation of our study.

Our findings suggest that FURIN inhibition may be beneficial for the inhibition of atherosclerosis and restenosis. The prevention of vascular MMP2 activation via FURIN inhibition may constitute an attractive mechanism to attenuate the development of severe lesions, and may lead to increased plaque stability, thus representing a new therapeutic option for the treatment of atherosclerosis. Since advanced lesions leading to plaque rupture is the primary driver for CAD-related mortality, this possibility may have far-reaching clinical consequences. Furthermore, due to FURIN's role as an upstream activator of multiple substrates, inhibiting FURIN is likely to provide a broader benefit in lesion development, compared to targeting individual downstream effectors.

Supplementary Material

Refer to Web version on PubMed Central for supplementary material.

Acknowledgements

We thank Wim van Duyvenvoorde and Marijke Voskuilen for excellent technical assistance in atherosclerotic lesion analyses and Roya Soltan, Melanie Garbe and Nadine Persigehl for their excellent technical assistance in tissue sample preparation and immunohistochemical staining. We certify that all persons who have made substantial contributions to the manuscript but who do not fulfill authorship criteria are named with their specific contributions in the Acknowledgments section of the manuscript, and that all persons named in the Acknowledgments section have provided the corresponding author with written permission to be named in the manuscript.

Sources of funding

The work in this manuscript was funded by the Singapore Ministry of Education Tier 2 grant (MOE2016-T2-1-122) to SG and RRS, as well as by the Agency for Science, Technology and Research and the National University of Singapore to RRS. HCF was supported by the Russian Government Program for competitive growth of Kazan Federal University, Kazan (Russian Federation), by the SHF-Foundation (SHF/FG657P/2017) and by the von Behring-Röntgen-Foundation (Marburg, Germany). DJH is supported by the Duke-National University Singapore Medical School; Singapore Ministry of Health's National Medical Research Council (NMRC/CSA-SI/0011/2017) and Collaborative Centre Grant (NMRC/CGAug16C006); the Singapore Ministry of Education Tier 2 (MOE2016-T2-2-021); National Institute for Health Research University College London Hospitals Biomedical Research Centre; and the British Heart Foundation (FS/10/039/28270). EAL was funded by the Interdisciplinary Center for Clinical Research IZKF Aachen (Junior Research Group E.A.L.). SG is supported by the American Heart Association (AHA10SDG4230068), the National Medical Research Council, Singapore, and the Ministry of Health, Singapore.

Abbreviations:

MMP2	matrix metalloproteinase 2
MMP9	matrix metalloproteinase 9
Ldlr	Low density lipoprotein receptor
ApoE	Apolipoprotein e
ASCVD	atherosclerotic cardiovascular disease
M-CSF	macrophage colony-stimulating factor
TGF-β	transforming growth factor beta
LPS	lipopolysaccharide

References:

1. Barquera S, Pedroza-Tobías A, Medina C, Hernández-Barrera L, Bibbins-Domingo K, Lozano R, Moran AE. Global overview of the epidemiology of atherosclerotic cardiovascular disease. *Arch Med Res.* 2015;46:328–338. doi: 10.1016/j.arcmed.2015.06.006. [PubMed: 26135634]
2. Cannon CP, Braunwald E, McCabe CH, Rader DJ, Rouleau JL, Belder R, Joyal SV, Hill KA, Pfeffer MA, Skene AM; Pravastatin or Atorvastatin Evaluation and Infection Therapy-Thrombolysis in Myocardial Infarction 22 Investigators. Intensive versus moderate lipid lowering with statins after acute coronary syndromes. *N Engl J Med.* 2004;350:1495–1504. DOI: 10.1056/NEJMoa040583 [PubMed: 15007110]
3. Preuss M, König IR, Thompson JR et al. Design of the Coronary ARtery Disease Genome-Wide Replication And Meta-Analysis (CARDIoGRAM) Study: A Genome-wide association meta-analysis involving more than 22,000 cases and 60,000 controls. *Circ Cardiovasc Genet.* 2010;3:475–483. doi: 10.1161/CIRCGENETICS.109.899443. [PubMed: 20923989]
4. Ghosh S, Vivar J, Nelson CP et al. Systems genetics analysis of genome-wide association study reveals novel associations between key biological processes and coronary artery disease.

- Arterioscler Thromb Vasc Biol. 2015;35:1712–1722. doi: 10.1161/ATVBAHA.115.305513. [PubMed: 25977570]
5. Roebroek AJ, Umans L, Pauli IG, Robertson EJ, van Leuven F, Van de Ven WJ, Constam DB. Failure of ventral closure and axial rotation in embryos lacking the proprotein convertase furin. *Development*. 1998;125:4863–4876. [PubMed: 9811571]
 6. Scamuffa N, Sfaxi F, Ma J, Lalou C, Seidah N, Calvo F, Khatib AM. Prodomain of the proprotein convertase subtilisin/kexin Furin (ppFurin) protects from tumor progression and metastasis. *Carcinogenesis*. 2014;35:528–536. doi: 10.1093/carcin/bgt345. [PubMed: 24127186]
 7. Bassi DE, Zhang J, Cenna J, Litwin S, Cukierman E, Klein-Szanto AJ. Proprotein convertase inhibition results in decreased skin cell proliferation, tumorigenesis, and metastasis. *Neoplasia*. 2010;12:516–526. [PubMed: 20651981]
 8. Lin H, Ah Kioon MD, Lalou C, Larghero J, Launay JM, Khatib AM, Cohen-Solal M. Protective role of systemic furin in immune response-induced arthritis. *Arthritis Rheum*. 2012;64:2878–2886. doi: 10.1002/art.34523. [PubMed: 22605541]
 9. Wylie JD, Ho JC, Singh S, McCulloch DR, Apte SS. Adamts5 (aggrecanase-2) is widely expressed in the mouse musculoskeletal system and is induced in specific regions of knee joint explants by inflammatory cytokines. *J Orthop Res*. 2012;30:226–233. doi: 10.1002/jor.21508. [PubMed: 21800360]
 10. Komiyama T, Swanson JA, Fuller RS. Protection from anthrax toxin-mediated killing of macrophages by the combined effects of furin inhibitors and chloroquine. *Antimicrob Agents Chemother*. 2005;49:3875–3882. DOI: 10.1128/AAC.49.9.3875-3882.2005 [PubMed: 16127065]
 11. Ozden S, Lucas-Hourani M, Ceccaldi PE et al. Inhibition of Chikungunya virus infection in cultured human muscle cells by furin inhibitors: impairment of the maturation of the E2 surface glycoprotein. *J Biol Chem*. 2008;283:21899–21908. doi: 10.1074/jbc.M802444200. [PubMed: 18559340]
 12. Stawowy P, Kallisch H, Stawowy NBP, Stibenz D, Veinot JP, Grafe M, Seidah NG, Chretien M, Fleck E, Graf K. Immunohistochemical localization of subtilisin/kexinlike proprotein convertases in human atherosclerosis. *Virchows Arch*. 2005;446:351–359. DOI: 10.1007/s00428-004-1198-7 [PubMed: 15756593]
 13. Stawowy P, Fleck E. Proprotein convertases furin and PC5: targeting atherosclerosis and restenosis at multiple levels. *J Mol Med (Berl)*. 2005;83:865–875. DOI: 10.1007/s00109-005-0723-8 [PubMed: 16244876]
 14. Lei X, Basu D, Li Z, Zhang M, Rudic RD, Jiang XC, Jin W. Hepatic overexpression of the prodomain of furin lessens progression of atherosclerosis and reduces vascular remodeling in response to injury. *Atherosclerosis*. 2014;236:121–130. doi: 10.1016/j.atherosclerosis.2014.06.015 [PubMed: 25026302]
 15. Fathy SA, Abdel Hamid FF, Zabut BM, Jamee AF, Ali MA, Abu Mustafa AM. Diagnostic utility of BNP, corin and furin as biomarkers for cardiovascular complications in type 2 diabetes mellitus patients. *Biomarkers*. 2015;20:460–469. doi: 10.3109/1354750X.2015.1093032. [PubMed: 26488448]
 16. CARDIoGRAMplusC4D Consortium, Deloukas P, Kanoni S et al. Large-scale association analysis identifies new risk loci for coronary artery disease. *Nat Genet*. 2013;45:25–33. doi: 10.1038/ng.2480. [PubMed: 23202125]
 17. Shiryayev SA, Remacle AG, Ratnikov BI et al. Targeting host cell furin proprotein convertases as a therapeutic strategy against bacterial toxins and viral pathogens. *J Biol Chem*. DOI: 10.1074/jbc.M703847200 2007;282:20847–20853. [PubMed: 17537721]
 18. Ma YC, Fan WJ, Rao SM, Gao L, Bei ZY, Xu ST. Effect of Furin inhibitor on lung adenocarcinoma cell growth and metastasis. *Cancer Cell Int*. 2014;14:43. doi: 10.1186/1475-2867-14-43. [PubMed: 24876827]
 19. Seidah NG, Prat A. The biology and therapeutic targeting of the proprotein convertases. *Nat Rev Drug Discov*. 2012;11:367–383. [PubMed: 22679642]
 20. Couture F, Kwiatkowska A, Dory YL, Day R. Therapeutic uses of furin and its inhibitors: a patent review. *Expert Opin Ther Pat*. 2015;25:379–396. doi: 10.1517/13543776.2014.1000303. [PubMed: 25563687]

21. Bassi DE, Lopez De Cicco R, Mahloogi H, Zucker S, Thomas G, Klein-Szanto AJ. Furin inhibition results in absent or decreased invasiveness and tumorigenicity of human cancer cells. *Proc Natl Acad Sci U S A*. 2001;98:10326–10331. DOI: 10.1073/pnas.191199198 [PubMed: 11517338]
22. Coppola JM, Bhojani MS, Ross BD, Rehemtulla A. A small-molecule furin inhibitor inhibits cancer cell motility and invasiveness. *Neoplasia*. 2008;10:363–370. [PubMed: 18392131]
23. Mathur R, Rotroff D, Ma J, Shojaie A, Motsinger-Reif A. Gene set analysis methods: a systematic comparison. *BioData Min*. 2018;11:8. doi: 10.1186/s13040-018-0166-8. [PubMed: 29881462]
24. Fabregat A, Jupe S, Matthews L, Sidiropoulos K, Gillespie M, Garapati P, Haw R, Jassal B, Korninger F, May B, Milacic M, Roca CD, Rothfels K, Sevilla C, Shamovsky V, Shorsler S, Varusai T, Viteri G, Weiser J, Wu G, Stein L, Hermjakob H, D'Eustachio P. The Reactome Pathway Knowledgebase. *Nucleic Acids Res*. 2018;46(D1):D649–D655. doi: 10.1093/nar/gkx1132. [PubMed: 29145629]
25. Daugherty A, Tall AR, Daemen MJAP, Falk E, Fisher EA, García-Cardena G, Lusis AJ, Owens AP, 3rd, Rosenfeld ME, Virmani R; American Heart Association Council on Arteriosclerosis, Thrombosis and Vascular Biology; and Council on Basic Cardiovascular Sciences. Recommendation on design, execution, and reporting of animal atherosclerosis studies: A scientific statement from the American Heart Association. *Arterioscler Thromb Vasc Biol*. 2017;37:e131–e157. doi: 10.1161/ATV.0000000000000062. [PubMed: 28729366]
26. Stary HC, Chandler AB, Dinsmore RE, Fuster V, Glagov S, Insull W, Jr, Rosenfeld ME, Schwartz CJ, Wagner WD, Wissler RW. A definition of advanced types of atherosclerotic lesions and a histological classification of atherosclerosis. A report from the committee on vascular lesions of the council on arteriosclerosis, american heart association. *Arterioscler Thromb Vasc Biol*. 1995;15:1512–1531. [PubMed: 7670967]
27. Stary HC, Chandler AB, Glagov S, Guyton JR, Insull W, Jr, Rosenfeld ME, Schaffer SA, Schwartz CJ, Wagner WD, Wissler RW. A definition of initial, fatty streak, and intermediate lesions of atherosclerosis. A report from the committee on vascular lesions of the council on arteriosclerosis, american heart association. *Arterioscler Thromb Vasc Biol*. 1994;14:840–856.
28. Simsekylmaz S, Cabrera-Fuentes HA, Meiler S, Kostin S, Baumer Y, Liehn EA, Weber C, Boisvert WA, Preissner KT, Zerneck A. Role of extracellular RNA in atherosclerotic plaque formation in mice. *Circulation*. 2014;129:598–606. doi: 10.1161/CIRCULATIONAHA.113.002562. [PubMed: 24201302]
29. Shagdarsuren E, Bidzhekov K, Djalali-Talab Y, Liehn EA, Hristov M, Matthijsen RA, Buurman WA, Zerneck A, Weber C. C1-esterase inhibitor protects against neointima formation after arterial injury in atherosclerosis-prone mice. *Circulation*. 2008;117:70–78. DOI: 10.1161/CIRCULATIONAHA.107.715649 [PubMed: 18071075]
30. Shagdarsuren E, Djalali-Talab Y, Aurrand-Lions M, Bidzhekov K, Liehn EA, Imhof BA, Weber C, Zerneck A. Importance of junctional adhesion molecule-C for neointimal hyperplasia and monocyte recruitment in atherosclerosis-prone mice-brief report. *Arterioscler Thromb Vasc Biol*. 2009;29:1161–1163. doi: 10.1161/ATVBAHA.109.187898. [PubMed: 19520977]
31. Ritz C, Baty F, Streibig JC, Gerhard D. Dose-Response Analysis Using R. *PLoS One*. 2015;10:e0146021. doi: 10.1371/journal.pone.0146021. [PubMed: 26717316]
32. Croft D, Mundo AF, Haw R et al. The Reactome pathway knowledgebase. *Nucleic Acids Res*. 2014;42:D472–477. doi: 10.1093/nar/gkt1102. [PubMed: 24243840]
33. Katsuda S, Kaji T. Atherosclerosis and extracellular matrix. *J Atheroscler Thromb*. 2003;10:267–274. [PubMed: 14718743]
34. Hu W, Huang Y. Targeting the platelet-derived growth factor signaling in cardiovascular disease. *Clin Exp Pharmacol Physiol*. 2015;42:1221–1224. doi: 10.1111/1440-1681.12478. [PubMed: 26277708]
35. Rizzo P, Ferrari R. The Notch pathway: A new therapeutic target in atherosclerosis? *Eur Heart J Supp*. 2015;17(A):74–76. doi: 10.1093/eurheartj/ehu244.
36. Toma I, McCaffrey TA. Transforming growth factor- β and atherosclerosis: interwoven atherogenic and atheroprotective aspects. *Cell Tissue Res*. 2012;347:155–175. doi: 10.1007/s00441-011-1189-3. [PubMed: 21626289]

37. Barrett T, Troup DB, Wilhite SE et al. NCBI GEO: archive for high-throughput functional genomic data. *Nucleic Acids Res.* 2009;37:D885–890. doi: 10.1093/nar/gkn764. [PubMed: 18940857]
38. Turpeinen H, Raitoharju E, Oksanen A, Oksala N, Levula M, Lyytikäinen LP, Järvinen O, Creemers JW, Kähönen M, Laaksonen R, Pelto-Huikko M, Lehtimäki T, Pesu M. Proprotein convertases in human atherosclerotic plaques: the overexpression of FURIN and its substrate cytokines BAFF and APRIL. *Atherosclerosis.* 2011;219:799–806. doi: 10.1016/j.atherosclerosis.2011.08.011. [PubMed: 21889147]
39. Garten W, Hallenberger S, Ortmann D, Schäfer W, Vey M, Angliker H, Shaw E, Klenk HD. Processing of viral glycoproteins by the subtilisin-like endoprotease furin and its inhibition by specific peptidylchloroalkylketones. *Biochimie.* 1994;76:217–25. [PubMed: 7819326]
40. Kim WJ, Essalmani R, Szumska D, Creemers JWM, Roebroek AJM, D'Orleans-Juste P, Bhattachary S, Seidah NG, Prat A. Loss of endothelial FURIN leads to cardiac malformation and early postnatal death. *Mol Cellular Biol.* 2012;32:3382–3391. doi: 10.1128/MCB.06331-11. [PubMed: 22733989]
41. Jean F, Stella K, Thomas L, Liu G, Xiang Y, Reason AJ, Thomas G. Alpha1-Antitrypsin Portland, a bioengineered serpin highly selective for furin: application as an antipathogenic agent. *Proc Natl Acad Sci U S A.* 1998;95:7293–7298. [PubMed: 9636142]
42. Breslow J Mouse models of atherosclerosis. *Science.* 1996;272:685–688. [PubMed: 8614828]
43. ten Dijke P, Arthur HM. Extracellular control of TGFbeta signalling in vascular development and disease. *Nat Rev Mol Cell Biol.* 2007;8:857–869. [PubMed: 17895899]
44. Shapiro MD, Fazio S. Apolipoprotein B-containing lipoproteins and atherosclerotic cardiovascular disease. *F1000Res.* 2017;6:134. doi: 10.12688/f1000research.9845.1. [PubMed: 28299190]
45. Stawowy P, Meyborg H, Stibenz D, Stawowy NBP, Roser M, Thanabalasingam U, Veinot JP, Chrétien M, Seidah NG, Fleck E, Graf K. Furin-like proprotein convertases are central regulators of the membrane type matrix metalloproteinase-pro-matrix metalloproteinase-2 proteolytic cascade in atherosclerosis. *Circulation.* 2005;111:2820–2827. [PubMed: 15911696]
46. Kuzuya M, Nakamura K, Sasaki T, Cheng XW, Itohara S, Iguchi. A Effect of MMP-2 deficiency on atherosclerotic lesion formation in apoE-deficient mice. *Arterioscler Thromb Vasc Biol.* 2006;26:1120–1125. [PubMed: 16556856]
47. Toth M, Fridman R. Assessment of gelatinases (MMP-2 and MMP-9) by gelatin zymography. *Methods Mol Med.* 2001;57:163–174. doi: 10.1385/1-59259-136-1:163. [PubMed: 21340898]
48. Wågsäter D, Zhu C, Björkegren J, Skogsberg J, Eriksson P. MMP-2 and MMP-9 are prominent matrix metalloproteinases during atherosclerosis development in the Ldlr(–/–) Apob(100/100) mouse. *Int J Mol Med.* 2011;28:247–53. doi: 10.3892/ijmm.2011.693. [PubMed: 21567073]
49. Luttun A, Lutgens E, Manderveld A, Maris K, Collen D, Carmeliet P, Moons L. Loss of matrix metalloproteinase-9 or matrix metalloproteinase-12 protects apolipoprotein E-deficient mice against atherosclerotic media destruction but differentially affects plaque growth. *Circulation.* 2004;109:1408–1414. DOI: 10.1161/01.CIR.0000121728.14930.DE [PubMed: 14993123]
50. Strongin AY, Collier I, Bannikov G, Marmer BL, Grant GA, Goldberg GI. Mechanism of cell surface activation of 72-kDa type IV collagenase. Isolation of the activated form of the membrane metalloprotease. *J Biol Chem.* 1995;270:5331–5338. [PubMed: 7890645]
51. Lindner V, Fingerle J, Reidy MA. Mouse model of arterial injury. *Circ Res.* 1993;73:792–796. [PubMed: 8403250]
52. Galis ZS, Sukhova GK, Lark MW, Libby P. Increased expression of matrix metalloproteinases and matrix degrading activity in vulnerable regions of human atherosclerotic plaques. *J Clin Invest.* 1994;94:2493–2503. DOI: 10.1172/JCI117619 [PubMed: 7989608]
53. Gough PJ, Gomez IG, Wille PT, Raines EW. Macrophage expression of active MMP-9 induces acute plaque disruption in apoE-deficient mice. *J Clin Invest.* 2006;116:59–69. DOI: 10.1172/JCI25074 [PubMed: 16374516]
54. McQuibban GA, Gong JH, Tam EM, McCulloch CA, Clark-Lewis I, Overall CM. Inflammation dampened by gelatinase A cleavage of monocyte chemoattractant protein-3. *Science.* 2000;289:1202–1206. [PubMed: 10947989]
55. Zhang K, McQuibban GA, Silva C, Butler GS, Johnston JB, Holden J, Clark-Lewis I, Overall CM, Power C. HIV-induced metalloproteinase processing of the chemokine stromal cell derived factor-1

- causes neurodegeneration. *Nat Neurosci.* 2003;6:1064–71. DOI: 10.1038/nn1127 [PubMed: 14502291]
56. Corry DB, Rishi K, Kanellis J, Kiss A, Song LZ, Xu J, Feng L, Werb Z, Kheradmand F. Decreased allergic lung inflammatory cell egression and increased susceptibility to asphyxiation in MMP2-deficiency. *Nat Immunol.* 2002;3:347–53. DOI: 10.1038/ni773. [PubMed: 11887181]
57. Tian S, Huang Q, Fang Y, Wu J. FurinDB: A database of 20-residue furin cleavage site motifs, substrates and their associated drugs. *Int J Mol Sci.* 2011;12:1060–1065. [PubMed: 21541042]
58. Benjannet S, Rhainds D, Hamelin J, Nassoury N, Seidah NG. The proprotein convertase (PC) PCSK9 is inactivated by furin and/or PC5/6A: functional consequences of natural mutations and post-translational modifications. *J Biol Chem.* 2006;281:30561–30572. DOI: 10.1074/jbc.M606495200 [PubMed: 16912035]
59. Cariou B, Le May C, Costet P. Clinical aspects of PCSK9. *Atherosclerosis.* 2011;216:258–265. DOI: 10.1016/j.atherosclerosis.2011.04.018 [PubMed: 21596380]
60. Cariou B, Ding Z, Mehta JL. PCSK9 and atherosclerosis: Beyond LDL-cholesterol lowering. *Atherosclerosis.* 2016;253:275–277. DOI: 10.1016/j.atherosclerosis.2016.08.007 [PubMed: 27591126]
61. Ferri N, Marchianò S, Tibolla G, Baetta R, Dhyani A, Ruscica M, Uboldi P, Catapano AL, Corsini A. PCSK9 knock-out mice are protected from neointimal formation in response to perivascular carotid collar placement. *Atherosclerosis.* 2016;253:214–224. DOI: 10.1016/j.atherosclerosis.2016.07.910 [PubMed: 27477186]
62. Anderson ED, Thomas L, Hayflick JS, Thomas G. Inhibition of HIV-1 gp160-dependent membrane fusion by a furin-directed α 1-antitrypsin variant. *J Biol Chem.* 1993;268:24887–24891. [PubMed: 8227051]
63. Essalmani R, Hamelin J, Marcinkiewicz J, Chamberland A, Mbikay M, Chrétien M, Seidah NG, Prat A. Deletion of the gene encoding proprotein convertase 5/6 causes early embryonic lethality in the mouse. *Mol Cell Biol.* 2006;26:354–361. DOI: 10.1128/MCB.26.1.354-361.2006 [PubMed: 16354705]
64. Molloy SS, Thomas G. Furin In: Dalbey RE, Sigman DS, eds. *The Enzymes*, Vol. XXII, 3rd Ed. San Diego, CA: Academic Press; 2002:199–235. 10.1016/S1874-6047(02)80009-9
65. Robinet P, Milewicz DM, Cassis LA, Leeper NJ, Lu HS, Smith JD. Consideration of sex differences in design and reporting of experimental arterial pathology studies-Statement from ATVB Council. *Arterioscler Thromb Vasc Biol.* 2018;38:292–303. doi: 10.1161/ATVBAHA.117.309524. [PubMed: 29301789]

Highlights

- Inhibition of FURIN *in vitro* reduced monocyte transmigration and macrophage and vascular endothelial cell inflammatory gene expression
- Inhibition of FURIN in a wire-injured *ApoE*^{-/-} model of vascular remodeling resulted in lower lesion area and lower intima thickening
- Inhibition of FURIN in western type diet fed *Ldlr*^{-/-} mice reduced severe atherosclerotic lesions
- Over expression of FURIN significantly increased intimal lesions in the wire injury model of atherosclerosis, confirming a direct role for FURIN in atherosclerosis.
- MMP2 activity is significantly lower in aortic arch of FURIN inhibitor treated mice, suggesting a contribution to lesion reduction.

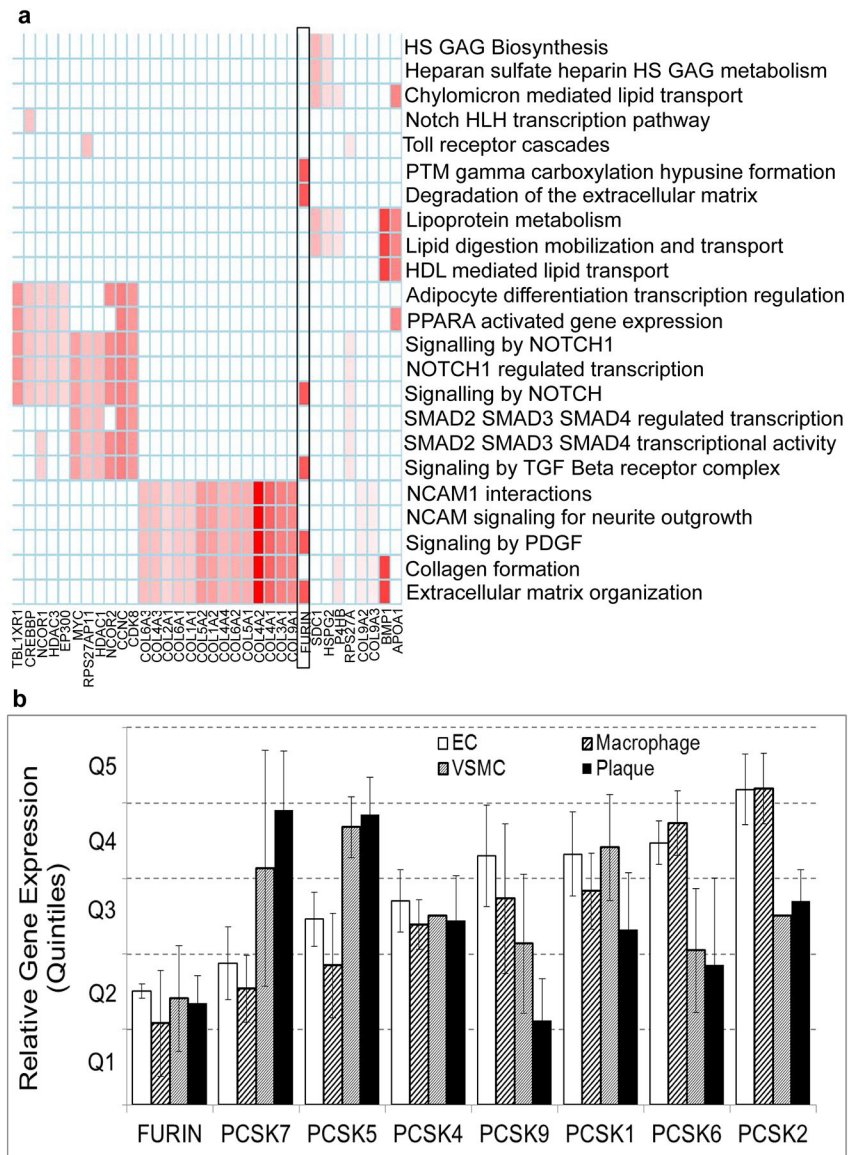


Figure 1: Genetic and genomic evidence for the association of *FURIN* with CAD.

(a) Heatmap representing genes that are common members of biological pathways significantly associated with CAD⁴. The results for *FURIN* are highlighted in the black-bordered rectangle. Heatmap is color-coded by the negative logarithm of the CAD-association p-values for the respective genes. **(b)** Expression of *FURIN* in genome-scale expression datasets in Gene Expression Omnibus. Expression of *FURIN* and other PCSKs were quantified in 570 samples encompassing vascular endothelial cells (EC), vascular smooth muscle cells (VSMC), monocyte/macrophages (Macrophage) and human atherosclerotic plaques (Plaque). To allow comparisons between disparate experiments, gene expression levels were converted to quantiles (quintiles) with quintile 1 (Q1) representing the top 20% expressed genes.

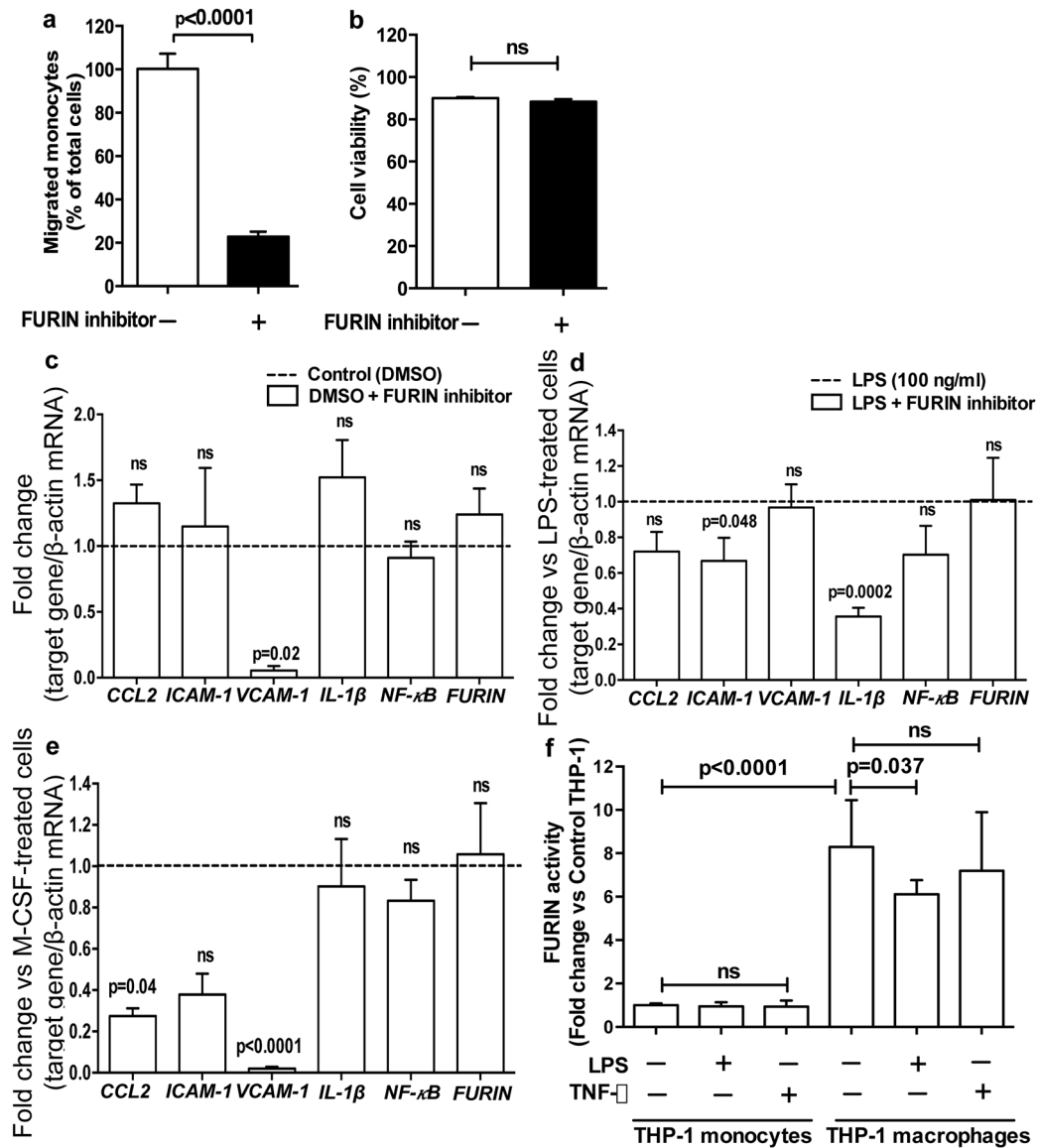


Figure 2: FURIN inhibition decreases monocyte migration and inflammatory gene expression *in vitro*.

(a) Activated human THP-1 monocytes were subjected to trans-well migration assays. In the presence of the FURIN inhibitor Dec-RVKR-CMK, a significantly lower number of monocytes migrated to the chemo-attractant M-CSF, and (b), the lower number of transmigrated monocytes did not result from increased cell death. (c) Lower *VCAM-1* expression level in FURIN inhibitor treated monocytes. (d) *ICAM-1* and *IL-1 β* transcription is significantly reduced in FURIN inhibitor treated monocytes upon LPS stimulation. (e) *CCL2* and *VCAM-1* transcription is significantly reduced in FURIN inhibitor treated M-CSF derived macrophages. (f) FURIN activity is significantly decreased in LPS-treated macrophages. Data represent mean \pm SEM of 3 independent experiments performed in triplicate. The dotted lines in (c), (d) and (e) represent control values. Data in a,b and f were assessed using Student's T-tests. Data in c-e used Kruskal-Wallis ANOVA tests.

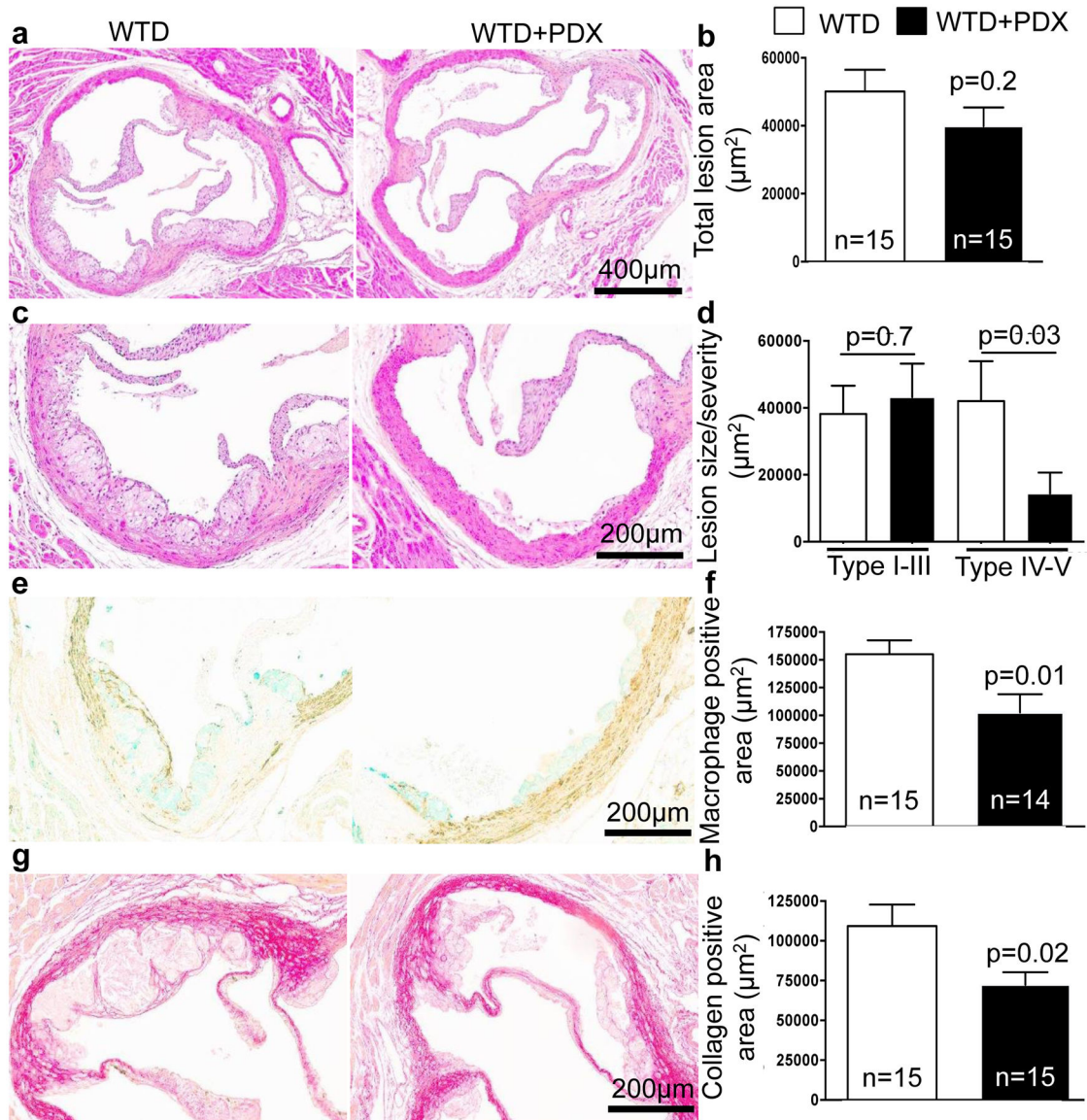


Figure 3: Lower lesion complexity and severe atherosclerotic lesion size in FURIN inhibitor treated mice.

(a) Representative photomicrographs of aortic sinus after histological staining with hematoxylin-phloxine-saffron (200x). (b) A trend toward lower aortic sinus lesion area in FURIN inhibitor treated mice. (c) Representative photomicrographs of lesion severity in aortic sinus after histological staining with hematoxylin-phloxine-saffron (100x). (d) Significantly lower severe lesion area (type IV and V) in FURIN inhibitor treated mice. (e) Representative photomicrographs of macrophages (green) in aortic sinus (100x). (f) Significantly lower lesional macrophage area in FURIN inhibitor treated mice. (g) Representative photomicrographs of aortic root after histological staining with picrosirius red for collagen (100x). (h) Significantly lower collagen area in lesions of FURIN inhibitor treated mice. Groups are abbreviated as: *Ldlr*^{-/-} mice fed Western type diet injected with PBS (WTD); *Ldlr*^{-/-} mice fed Western type diet injected with the α -1-PDX FURIN inhibitor (WTD+PDX). All mice are male. Values represent mean \pm SEM. Data in f and h

are normally distributed, and p-values were assessed using Student's T-tests. Data in **b** and **d** were not normally distributed, and Mann-Whitney tests were used.

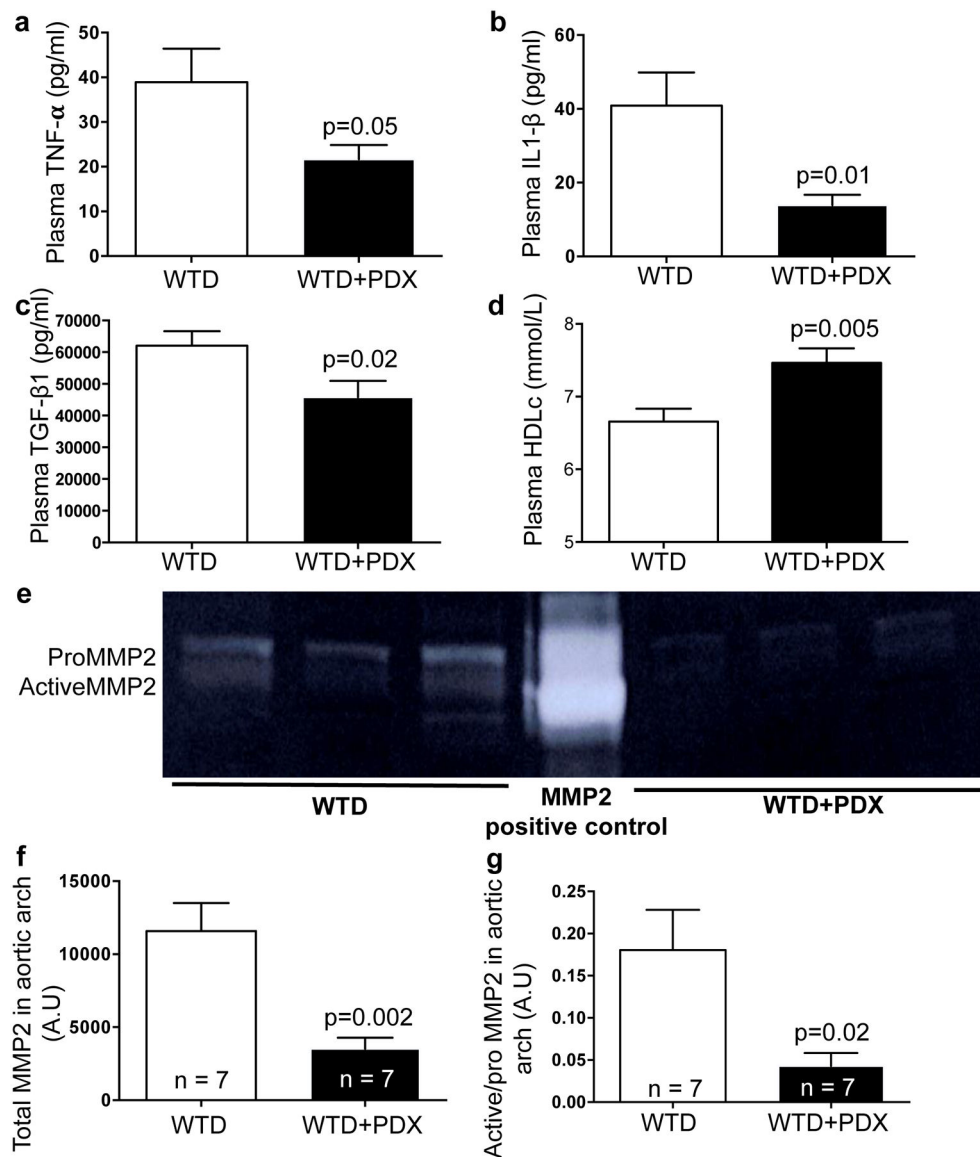


Figure 4: Lower plasma inflammatory markers, elevated plasma HDL cholesterol and lower MMP2 expression in aorta of FURIN inhibitor treated mice.

Lower plasma levels of (a) TNF- α , (b) IL1- β , (c) TGF- β 1, and (d) elevated plasma HDL cholesterol levels in FURIN inhibitor treated mice. n=14–16 for all analyses. (e) Gelatin zymography in the aortic arch showing both the pro and active forms of MMP2. (f) Total MMP2 expression levels are significantly lower in the aortic arch of FURIN inhibitor treated mice. (g) Significantly lower active MMP2/proMMP2 expression in the aortic arch of FURIN inhibitor treated mice. Groups are abbreviated as: *Ldlr*^{-/-} mice fed Western type diet injected with PBS (WTD); *Ldlr*^{-/-} mice fed Western type diet injected with the α -1-PDX FURIN inhibitor (WTD+PDX). A.U.= Arbitrary Units. Values represent mean \pm SEM. All mice are male. Data in a-f are normally distributed, and p-values were assessed using Student's T-tests. Data in g are not normally distributed, and Mann-Whitney test was performed.

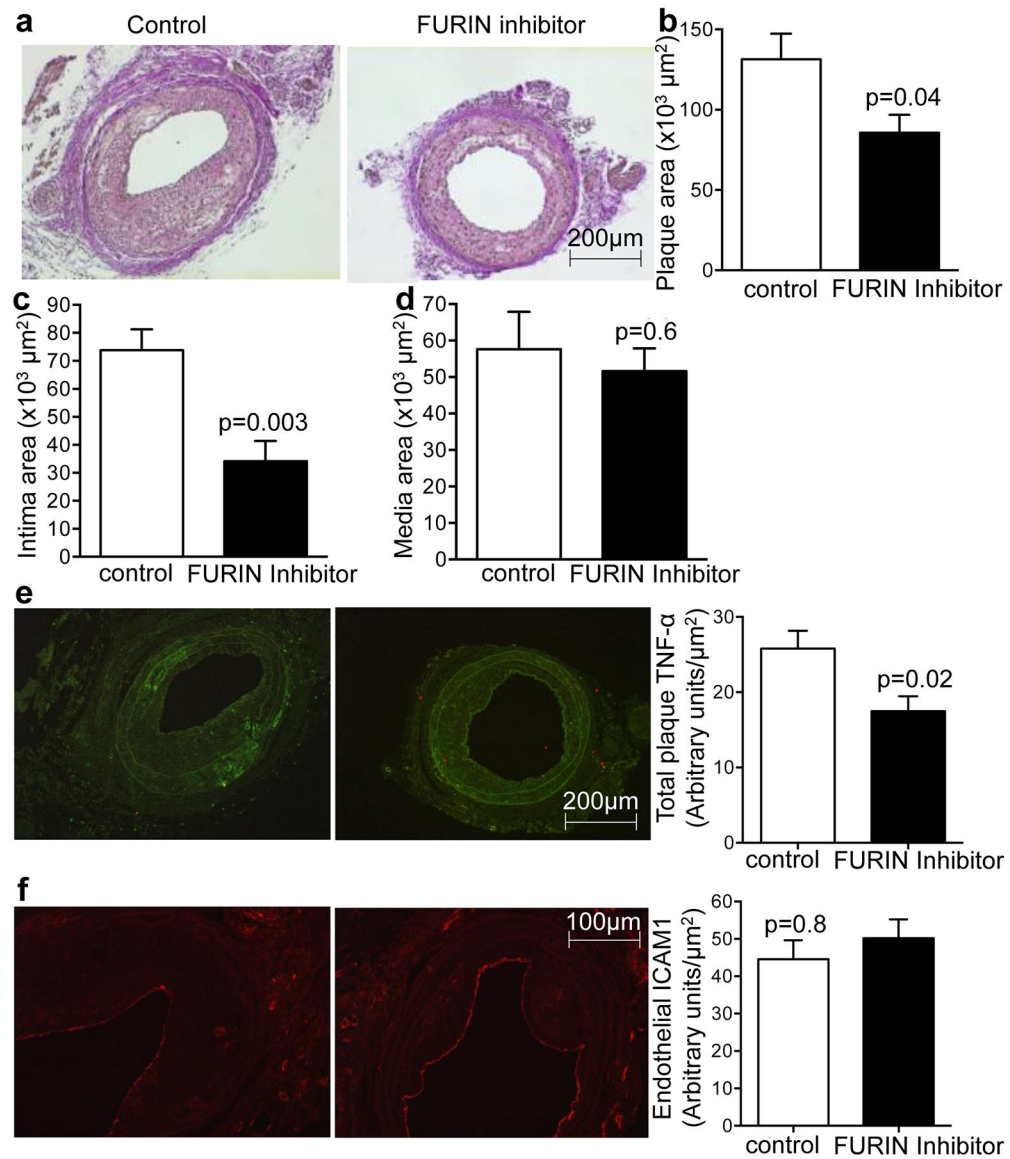


Figure 5: FURIN inhibition reduces neointimal plaque formation and inflammation in a wire injury model of atherosclerosis. Male *Apoe*^{-/-} mice were fed a high-fat diet, treated with vehicle (DMSO) or FURIN Inhibitor α -1-PDX and were subjected to wire injury of the common carotid artery. **(a)** Representative photomicrographs of pentachrome-stained sections 2 weeks after injury, **(b)** Significantly lower plaque area, **(c)** Significantly lower neointima area, and **(d)** Unchanged media area in FURIN inhibitor treated mice. **(e)** Significantly decreased vascular inflammatory cytokine TNF- α levels (stained in green), and **(f)** Unchanged endothelial adhesion molecule ICAM1 levels (stained in red) in FURIN inhibitor treated mice. Groups are abbreviated as: *Apoe*^{-/-} mice (Control); *Apoe*^{-/-} mice administered the FURIN inhibitor α -1-PDX (FURIN inhibitor). n=6 per group. Values represent mean \pm SEM. Data in **a-e** are normally distributed, and p-values were assessed using Student's T-tests. Data in **f** was not normally distributed and a Mann-Whitney test was used.

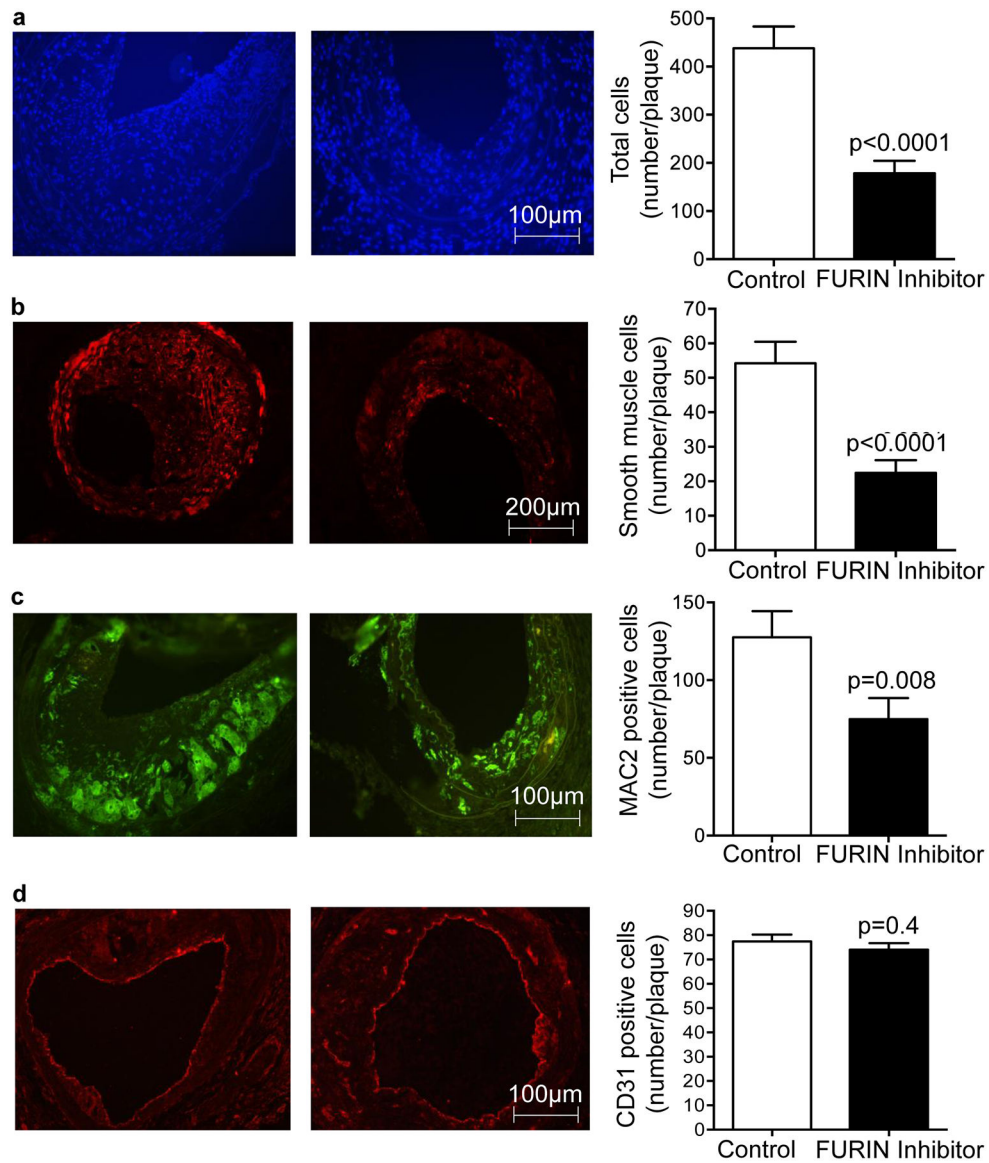


Figure 6: FURIN inhibition reduces plaque complexity in a wire injury model of atherosclerosis. Male *Apoe*^{-/-} mice were fed a high-fat diet, treated with vehicle (control) or FURIN Inhibitor α -1-PDX and subjected to wire-induced injury of the common carotid artery. (a) The total number of cells, (b) the number of smooth muscle cells, and (c) the number of MAC2 positive macrophages per plaque were all significantly lower in FURIN inhibitor treated mice. (d) No changes in CD31⁺ endothelial cell numbers were observed. Groups are abbreviated as: *Apoe*^{-/-} mice (Control); *Apoe*^{-/-} mice administered the FURIN inhibitor α -1-PDX (FURIN inhibitor). n=6 per group. Values represent mean \pm SEM. Data in a-c are not normally distributed, and p-values were assessed using Mann-Whitney tests. Data in d is normally distributed, and Student's T-test was used.

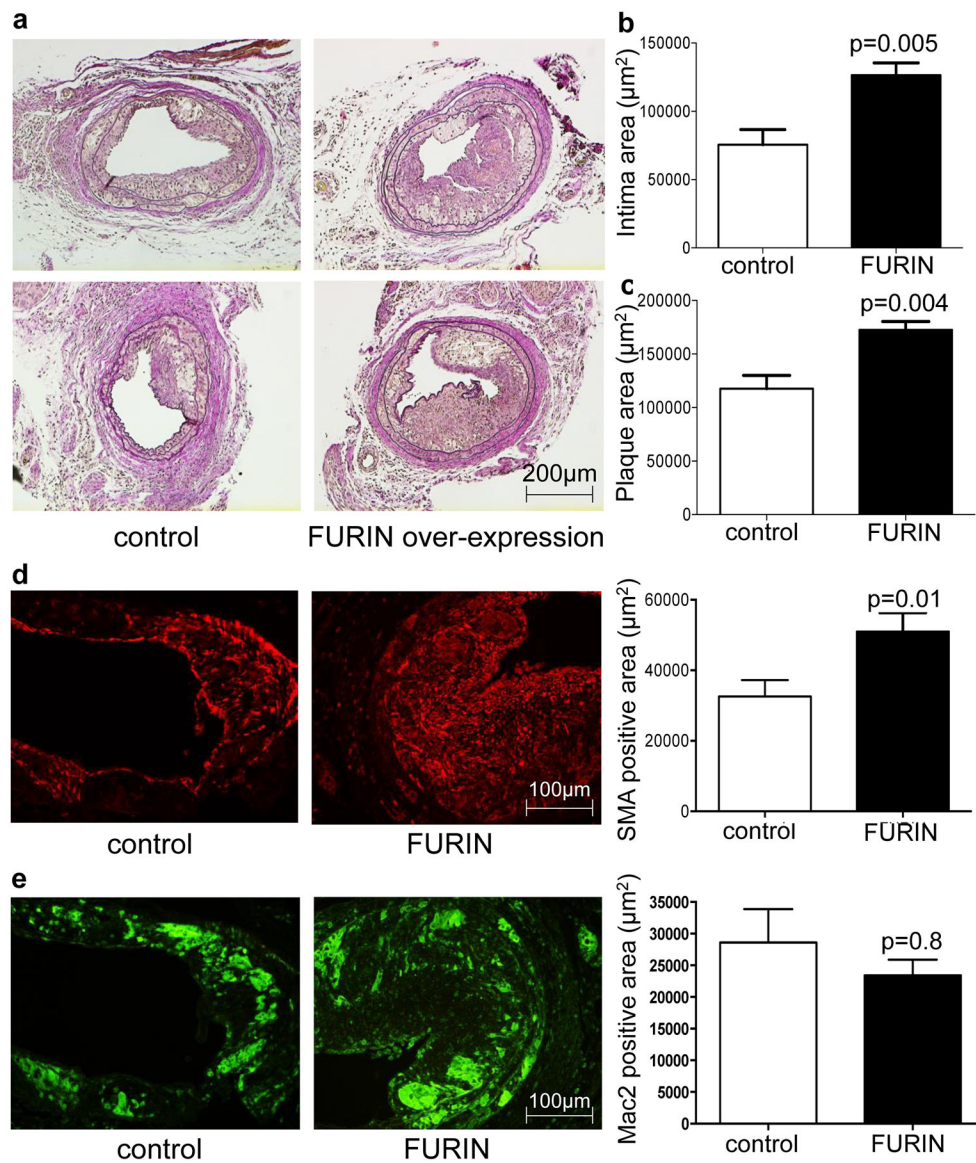


Figure 7: FURIN over-expression increases neointimal plaque formation in a wire injury model of atherosclerosis.

Male *Apoe*^{-/-} mice were fed a western-type diet, subjected to wire-induced injury of the common carotid artery, and treated with vehicle (n=5) or purified FURIN protein (n=6). (a) Representative photomicrographs of pentachrome-stained sections at 2 weeks after injury, and (b) significantly higher neointima and (c) plaque area in FURIN protein injected mice. (d) Significantly increased smooth muscle cell area (stained in red), and (e) no change in macrophage area (stained in green) in the lesions of FURIN over-expressing mice. Groups are abbreviated as: *Apoe*^{-/-} mice (Control); *Apoe*^{-/-} mice administered purified FURIN protein (FURIN). Values represent mean ± SEM. Data in a-d are normally distributed, and p-values were assessed using Student's T-tests. Data in e is not normally distributed, and the Mann-Whitney test was used.